Serum Lipoprotein Structure: Resonance Energy Transfer Localization of Fluorescent Lipid Probes†

Larry A. Sklar,* Michael C. Doody, Antonio M. Gotto, Jr., and Henry J. Pownall‡

ABSTRACT: The location of several fluorescent chromophores in lipoproteins has been determined by using resonance energy transfer. The primary acceptor is 5-(*N*-hexadecanoylamino)fluorescein whose chromophore is shown to reside at the lipoprotein surface at pH 7.4. Polar donors include *cis*-parinaric acid (*cis,trans,trans,cis*-9,11,13,15-octadecatetraenoic acid), *trans*-parinaric acid (*all-trans*-9,11,13,15-octadecatetraenoic acid), and 16-(9-anthroyloxy)palmitic acid; nonpolar donors are parinaric acid methyl ester, parinaric acid cholesteryl ester, and 1,6-diphenyl-1,3,5-hexatriene. The polar donors transfer more efficiently than the nonpolar donors in several classes of lipoprotein particles. The data are analyzed by a simple mathematical model from which it is concluded that the polar donors are localized in the putative lipoprotein surface monolayer; the possibility that nonpolar donors are partitioned between the surface and core of lipoproteins is considered.

Resonance energy transfer promises to be an effective means of studying the organization of macromolecular structures particularly if their sizes and shapes are already known. This paper develops an approach for the application of resonance energy transfer to the structure of serum lipoproteins. Prior to the recent evaluation of theoretical expressions to analyze energy transfer on surfaces (Fung & Stryer, 1978; Wolber & Hudson, 1979) or spherical particles (Doody et al., 1979), a quantitative analysis of energy transfer in lipoproteins was not possible (Smith & Green, 1974; Jonas, 1977). These mathematical methods which treat energy transfer in a number of cases relevant to lipoprotein organization will be considered elsewhere.[1]

Since lipoproteins are generally viewed as a surface layer of polar lipid and protein surrounding a core of nonpolar lipids [e.g., Shen et al. (1977)], we have designed an experimental strategy particularly suited to these structural features. This approach differs in several important respects from the innovative studies of Fung & Stryer (1978) on energy transfer between chromophores on the surfaces of planar phospholipid bilayers, primarily because our probes can be readily introduced into intact biological structures. Our aim is to locate several lipid analogue fluorescent probes with respect to the lipoprotein surface by resonance energy transfer. We use both polar and nonpolar chromophores as shown in Chart I.

As a fluorescence acceptor, we use the slightly water-soluble lipid analogue 5-(*N*-hexadecanoylamino)fluorescein (I, HAF),[2] which binds quantitatively to lipoproteins under conditions defined here. HAF is shown by spectroscopic methods to be located at the lipoprotein surface. As donors, we use primarily lipids derived from the natural product polyene fatty acids *trans*-parinaric acid (II, *trans*-PnA) and *cis*-parinaric acid (III, *cis*-PnA) which have been extensively characterized in both biological and model systems (Sklar et al., 1975, 1977a,b, 1979b; Tecoma et al., 1977; Rintoul & Simoni, 1978; Berde et al., 1979). In addition, we have compared energy transfer from two other well-known probes, 16-(9-anthroyloxy)palmitic acid (IV, AP) and diphenylhexatriene (VII, DPH). The location of these donors is assigned on the basis of the efficiency of transfer to the surface acceptor. In a subsequent paper we will apply these methods to the organization of cholesteryl esters in LDL.[3] Energy transfer methods using donors and acceptors of nonpartitioning probes (such as those covalently bound to apo-B functional groups) or slowly redistributing probes (such as fluorescent lipid analogues including phospholipid, triglyceride, and cholesteryl ester) may prove sensitive to lipoprotein structural transformation arising from lipolysis, lipid exchange, or the interaction of lipoproteins with cells.

Materials and Methods

Fluorescent Probes. The isomers of parinaric acid (II and III) and their methyl esters (V) were prepared and stored in ethanolic stock solutions as described elsewhere (Sklar et al., 1977a, 1979b). Cholesteryl parinarate esters (VI) were prepared by a catalytic procedure described elsewhere (Patel et al., 1979). HAF (I) and AP (IV) were generous gifts of Dr. Richard Haugland of Molecular Probes, Inc., Plano, TX. The purity of HAF was confirmed by silicic acid thin-layer chromatography developed in 9:1 chloroform–methanol. Scintillation-grade DPH was obtained from Eastman.

Lipoproteins. Human VLDL was obtained from a patient with Type V hyperlipoproteinemia and subfractionated in a zonal rotor by Dr. Josef Patsch (Patsch et al., 1978). Human LDL (*d* 1.025–1.050 g/mL) was obtained from normal human donors by either sequential or zonal ultracentrifugation.

† From the Department of Medicine, Baylor College of Medicine and The Methodist Hospital, Houston, Texas 77030. *Received September 4, 1979.* This work was supported by grants from the National Institutes of Health (HL19459), the National Heart and Blood Vessel Institute Research and Demonstration Center (HL17269), and the American Heart Association to H.J.P. A preliminary account of this work was presented at the 1979 Biophysical Society meeting (Sklar et al., 1979a; Doody et al., 1979).

* Correspondence should be addressed to this author at the Department of Immunopathology, Scripps Clinic and Research Foundation, La Jolla, CA 92037. He is a Helen Hay Whitney Postdoctoral Fellow.

‡ Established Investigator of the American Heart Association.

[1] M. C. Doody, L. A. Sklar, A. M. Gotto, Jr., H. J. Pownall, and L. C. Smith, unpublished calculations. The algorithm should have the form $Q \approx 1 - \sum_i F_i \tau_i$ (Doody et al., 1979).

[2] Abbreviations used: AP, 16-(9-anthroyloxy)palmitic acid; CER-VLDL, cholesteryl ester rich very low density lipoprotein from cholesterol-fed rabbit; *cis*-PnA, *cis*-parinaric acid (*cis,trans,trans,cis*-9,11,13,15-octadecatetraenoic acid); DPH, diphenylhexatriene; HAF, 5-(*N*-hexadecanoylamino)fluorescein; HDL, human high density lipoprotein; LDL, human low density lipoprotein; *trans*-PnA, *trans*-parinaric acid (*all-trans*-9,11,13,15-octadecatetraenoic acid); VLDL, human very low density lipoprotein.

[3] L. A. Sklar, I. F. Craig, and H. J. Pownall, unpublished experiments.

0006-2960/80/0419-1294$01.00/0

Chart I

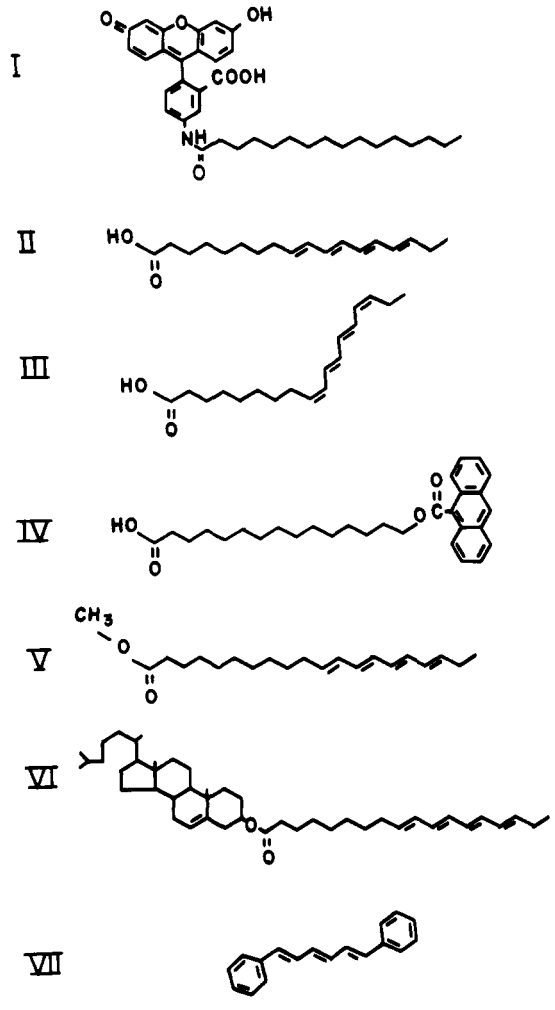

CER-VLDL, obtained from cholesterol-fed rabbits, was the gift of Dr. Joel Morrisett. CER-VLDL's were fractionated according to size by gel permeation chromatography.[4] Model VLDL particles, "triglyceride-rich dispersions" (60% triolein, 22% dipalmitoylphosphatidylcholine, 7% cholesterol, and 11% cholesterol myristate), were prepared by Dr. Steven Charlton and Gerald W. Jacobs by a 2-propanol injection procedure (Charlton et al., 1978).

Preparation of Samples for Fluorescence Measurements. Lipoprotein solutions (0.03–0.3 mg/mL total weight) were prepared on the basis of a calculation of the total surface area of the particles in the sample. Concentrations were picked so that an appropriate range of acceptor surface density could be achieved without exceeding inner and outer filter absorbance corrections of about 15%. Surface areas were calculated from the known size ranges of the particles and their known composition (Shen et al., 1977; Patsch et al., 1978). In most cases, the particle concentrations were based on their protein content as determined by the method of Lowry et al. (1951) in the presence of sodium dodecyl sulfate using a bovine serum albumin standard. Fluorescent probes except cholesteryl parinarate were incorporated into lipoprotein samples by injection of microliter aliquots of dilute ethanolic probe stock solutions into buffer (150 mM NaCl, 10 mM Hepes, 0.1% EDTA, and 0.01% NaN_3, pH 7.4) containing appropriate concentrations of lipoproteins. The samples were incubated at 37 °C until the fluorescence intensity reached its maximum (<10 min). Final ethanol concentrations were usually 0.1% or less by volume. Prior to energy transfer measurements, the samples were sealed under argon in their fluorescence cuvettes.

Sample concentrations were chosen so that HAF was bound over an appropriate range of surface densities as described in the legends to Figures 6 and 7. Surface areas were calculated by using the following lipoprotein structure–composition data: for LDL, a radius of 96 Å and 21% protein by weight (Shen et al., 1977); for VLDL, 275 Å and 5.2% protein (zonal subfraction 1, see the legend to Figure 8); for the model VLDL particles, a radius of 325 Å was determined by electron microscopy (S. Charlton, personal communication), and the total mass and surface area in the sample were calculated assuming the particle density equal to 1.0 g/mL; for rabbit CER-VLDL (Morrisett et al., 1979), the size was determined by laser light scattering (Morrisett et al., 1974), and total compositional analyses were provided by Dr. Joel Morrisett.

Spectroscopy. Absorption spectra were recorded on a Cary 14 scanning spectrophotometer. Fluorescence measurements were made on an SLM Model 8000 photon counting spectrofluorometer. In measurements of fluorescence energy transfer, emission spectra were recorded in duplicate at each acceptor concentration. Conditions were chosen to minimize probe bleaching by using a narrow excitation slit (0.5 nm) or neutral density filter in the excitation beam and a wide (8-nm) emission slit. Slight bleaching of PnA probes (less than 5%) and no bleaching of DPH or AP were observed over the course of an experiment. Absorption spectra were recorded for each sample so that inner filter and outer filter effects could be taken into account (Pesce et al., 1971). These corrections never exceed 15%.

Fluorescence quantum yields were calculated by comparing the fluorescence intensities at the emission maximum of probe-containing lipoprotein samples to known quantum yield standards with similar or identical emission spectra. PnA probes were compared to *cis*-PnA in ethanol at 25 °C (quantum yield equals 0.020; Sklar et al., 1977a); DPH and AP were compared to DPH in benzene (quantum yield equals 0.80; Berlman, 1971). Determinations were made under the conditions described in Figure 7: 0.308 mg/mL total LDL with ~10 probe molecules per LDL; quantum yields are essentially independent of probe concentrations at this low probe concentration. LDL concentrations are chosen so that donor probes are ~90% or greater bound (Sklar et al., 1979b); since the aqueous fluorescence of the donors is negligible, the presence of a small fraction of donors in the aqueous phase does not influence the energy transfer measurements.

Theory. Energy transfer efficiency (T) is calculated from the reduction of the emission of the donor according to the relationship

$$T = 1 - Q_A/Q_0 \quad (1)$$

where Q_0 refers to the unquenched quantum yield of the donor and Q_A refers to its quantum yield at a particular surface density of acceptor.

The acceptor surface density is expressed in terms of the number of acceptors per unit surface area, R_0^2 (Wolber & Hudson, 1979), where R_0 is the distance at which energy transfer between a particular donor–acceptor pair is 50%. R_0 is calculated according to

$$R_0 = (JQ_0K^2/n^4)^{1/6}(9.79 \times 10^3 \text{ Å}) \quad (2)$$

where K^2 is the dipole–dipole orientation factor, n is the refractive index of the medium, and J is the donor–acceptor spectral overlap integral in $cm^3\ M^{-1}$ (Table I). If energy

[4] J. D. Morrisett, unpublished experiments.

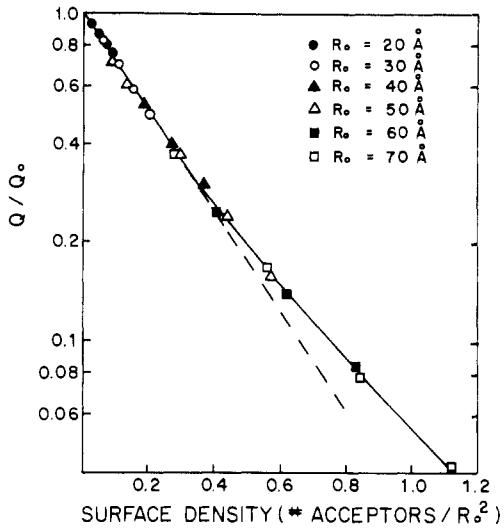

FIGURE 1: Energy transfer in a plane. Calculated data are plotted as Q_A/Q_0 on a logarithmic scale vs. the acceptor surface density expressed as the number of acceptors per R_0^2. Data are replotted from Fung & Stryer (1978, Figure 2). The data were originally plotted as the number of acceptors per phospholipid, in which case different R_0 values yield individual curves.

transfer is plotted as log (Q_A/Q_0) vs. the number of acceptors per R_0^2, the resulting plot is nearly linear over a range of experimentally accessible surface densities and the slope of the plot is independent of R_0 (Wolber & Hudson, 1979). These observations are summarized in Figure 1 in which calculations of Fung & Stryer (1978) are replotted.

We calculate the energy transfer for a number of cases relevant to lipoprotein structure by a method described elsewhere (Doody et al., 1979).[1] The method applies an algorithm which converges to the exact transfer efficiency at low acceptor surface density and which is extrapolated to higher surface densities by an exponential reduction of the donor quantum yield. This approach is valid, as shown in Figures 1 and 2 up to surface densities of at least 0.5 acceptor per R_0^2. Energy transfer calculated as a function of the depth of the donor chromophore from the surface is shown in Figure 2A for a plane and in Figure 2B,C for a spherical particle the size of a small LDL (radius 96 Å). The slopes of these plots are related to the depth of donors from the surface. Our calculations for a plane are compared to results obtained by Wolber & Hudson (1979) (Figure 2A). Essentially, we calculate a tangent to the initial slope of the Wolber–Hudson treatment. Differences between the exact and approximate treatment are on the order of 5% at surface densities of 0.5 acceptor per R_0^2. If, for example, R_0 is 30 Å and the area of a lipid is 60 Å^2, this represents 1 acceptor per 30 lipid molecules, a relatively high surface density. Although energy transfer does not distinguish well between depths of 0–0.6R_0 (there is only a 50% difference in slope from a depth of 0R_0), there is approximately a twofold decrease in slope for each increase in depth from 0.6- to 0.8- to 1.0R_0.

Results for two different R_0 values, in particles of radius equal to 96 Å, representing small LDL, are shown in parts B and C of Figure 2. The R_0 values selected, 27 or 42 Å, represent typical values for PnA donors (II, III, V, and VI) or AP (IV) and DPH (VII) donors, respectively (Table I). We observe that the calculated slopes depend upon R_0 due to the particle curvature: for example, a depth of 0.6R_0 in the plane (Figure 2A) corresponds to ~22 Å (or ~0.8R_0) for PnA in LDL (Figure 2B) and corresponds to 41 Å or ~1R_0 for AP or DPH (Figure 2C) in LDL. As the magnitude of R_0 approaches the particle radius, it becomes increasingly difficult

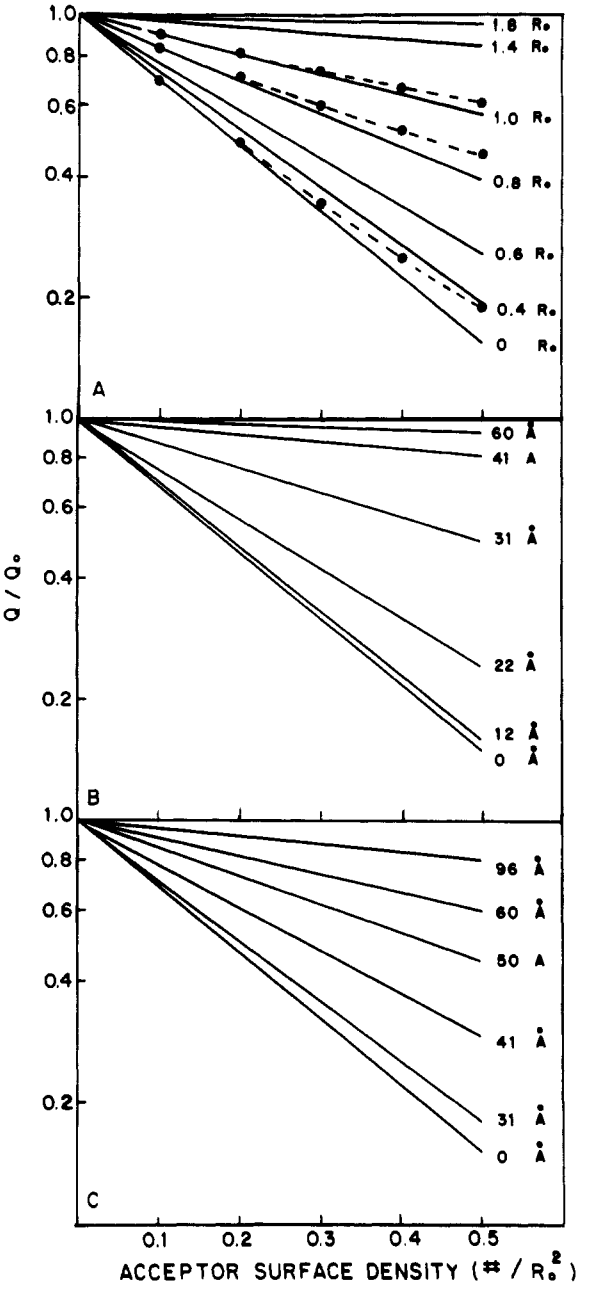

FIGURE 2: Energy transfer as a function of depth of donor from surface acceptor. Data are plotted as in Figure 1. (A) Energy transfer in a plane calculated according to Wolber & Hudson (●---●) (1979) and Doody et al. (—) (1979). Depths are expressed in terms of R_0. (B) Energy transfer in a spherical particle; radius = 192 Å; R_0 = 27 Å. (C) Energy transfer in a spherical particle; radius = 192 Å; R_0 = 42 Å. Depths (angstroms) are calculated according to Doody et al. (1979).

to distinguish donors on or just below the surface. Such a case occurs with a small lipoprotein such as HDL. However, when both donors and acceptors are on or near the surface (i.e., 0.0R_0 depth), energy transfer is very similar in a spherical particle or on a monolayer (i.e., nearly independent of curvature) even when the magnitude of R_0 approaches the particle radius. Fung & Stryer (1978) reached similar conclusions on energy transfer in a spherical monolayer.

Results

Binding of HAF by LDL. The absorption spectrum of HAF in aqueous buffer, pH 7.4, is shown as a function of concentration (Figure 3A). Above 2 μM, a characteristic sharp absorption band (λ_{max} = 513 nm), probably representing ex-

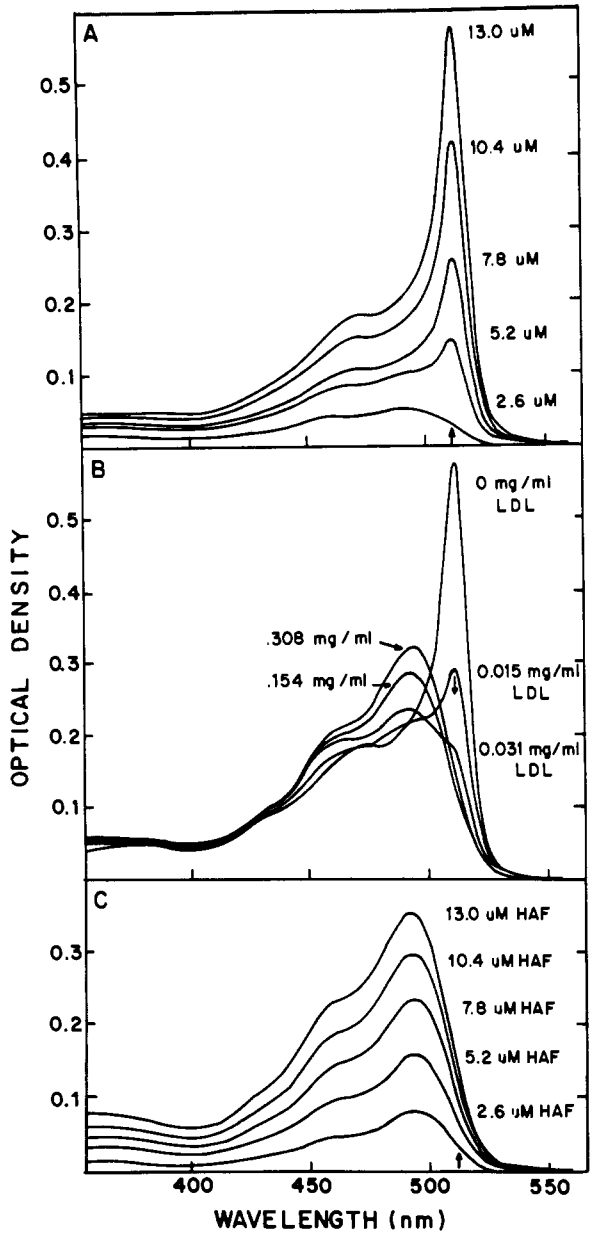

FIGURE 3: Binding of HAF to LDL by absorption spectroscopy. The absorption spectrum of HAF in buffer is shown as a function of HAF concentration (0–13 μM) (A). The absorption spectrum of HAF (13 μM) bound to LDL is shown as a function of LDL concentration (0–0.31 mg/mL total concentration) (B). The absorption spectrum of HAF bound to LDL (0.31 mg/mL) is shown as a function of the HAF concentration (0–13 μM) (C). Note that the concentration dependence of the absorbance is slightly nonlinear.

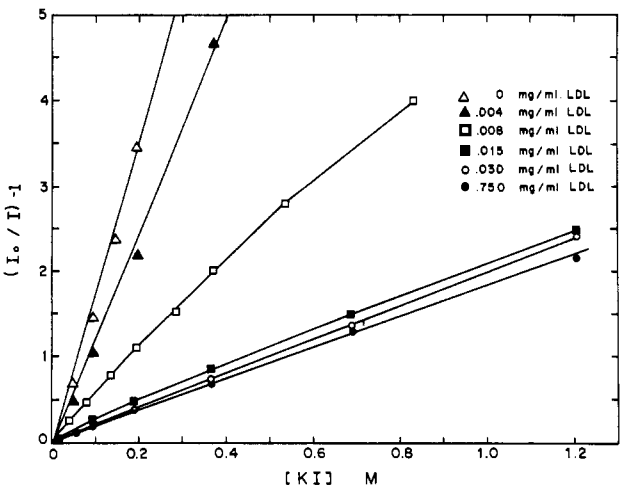

FIGURE 4: Stern–Volmer plot of the quenching of the fluorescence of HAF by aqueous iodide as a function of the concentration of LDL. The HAF concentration in the buffer was 1 μM. A freshly prepared stock solution of 5 M potassium iodide (containing 0.1% $K_2S_2O_3$) was added to samples containing various amounts of LDL (total milligrams per milliliter is shown in the figure). HAF was excited at 490 nm, and emission spectra were recorded as a function of iodide concentration.

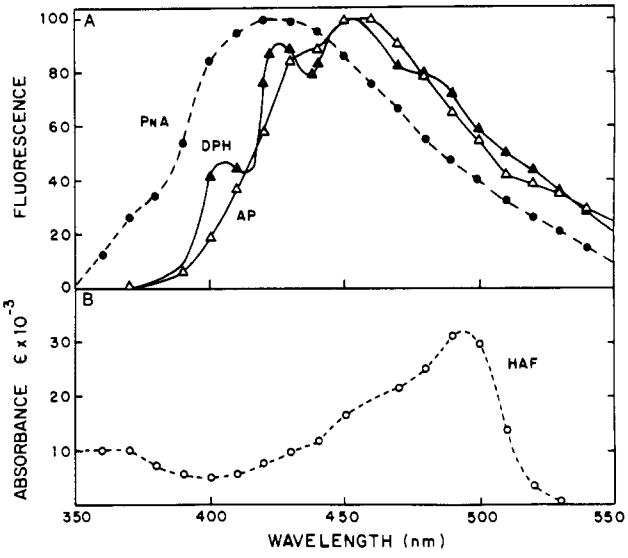

FIGURE 5: Spectral overlap of donor and acceptor chromophores. The corrected emission spectra of PnA (Sklar et al., 1977a), DPH (Berlman, 1971) and AP are plotted in (A). Spectral data for AP in LDL were obtained on the SLM 8000 with appropriate instrumental correction factors. The absorption spectrum of HAF is plotted in (B); extinction coefficients (ϵ) are based on the spectrum obtained at 2.6 μM (Figure 3C).

citonic interaction of the chromophore in micelles, is observed. This absorption band disappears when HAF binds to LDL (Figure 3B,C). For most experiments, the LDL concentration will exceed by a factor of 10 that concentration required to reduce the aqueous HAF (as indicated by the 513-nm band) to 50% of its original value (Figure 3B). That is, under most experimental conditions, HAF will be on the order of 90% bound. The absence of the 513-nm absorption band is our criterion for lack of significant aqueous HAF.

Evidence for the location of the HAF chromophore in LDL is derived from the Stern–Volmer plots of the quenching of HAF by aqueous iodide (Figure 4). Aqueous HAF (1 μM; i.e., below its critical micelle concentration) is readily accessible to quenching by iodide. When the LDL concentration is sufficiently high to bind all the HAF (see Figure 3B; 0.03 mg of LDL per mL), the quenching constant is reduced by at least a factor of 10. Further increases in LDL concentration have no effect on the quenching.

Spectral Overlap of HAF with Fluorescent Donors. Corrected emission spectra of the donor chromophores are presented in Figure 5A and compared to the absorption spectrum of the acceptor, HAF, in Figure 5B. The emission spectrum of PnA donors is independent of the derivative used, and there are only small differences between the cis and trans isomers (Sklar et al., 1977a). Values of R_0, the distance at which energy transfer for a given donor–acceptor pair is calculated to be 50%, for several typical experimental conditions are summarized in Table I. Spectral overlap integrals for all of the donor–acceptor pairs are similar, but the large differences in quantum yield between the PnA probes and either DPH or AP result in substantial differences in calculated R_0 values. For DPH and AP, R_0 values are near 42 Å. Since the

Table I: Spectral Parameters for Calculation of R_0 with Donors II–VII and (Hexadecanoylamino)fluorescein as the Acceptor[a]

donor	lipoprotein	Q	$J \times 10^{16}$ (cm^3/M)	R_0 (Å)
PnA	LDL, 10 °C	0.15	5.0	30.0
PnA	LDL, 25 °C	0.09	5.0	28.4
PnA	LDL, 37 °C	0.06	5.0	26.6
AP	LDL, 37 °C	0.6	7.2	41.5
DPH	LDL, 37 °C	0.8	6.8	43.0

[a] R_0 is the distance at which energy transfer between a single donor and acceptor is 50% and is defined as in eq 2. Q, the donor quantum yield, is determined as described under Materials and Methods. J, the spectral overlap integral, is illustrated in Figure 5 and calculated as in Fung & Stryer (1978). The orientation factor, K^2, is assumed to be 2/3 [see Haas et al. (1978)] and will be discussed in detail elsewhere.[3] The refractive index, n, is determined from the PnA absorption maximum (Sklar et al., 1977b).

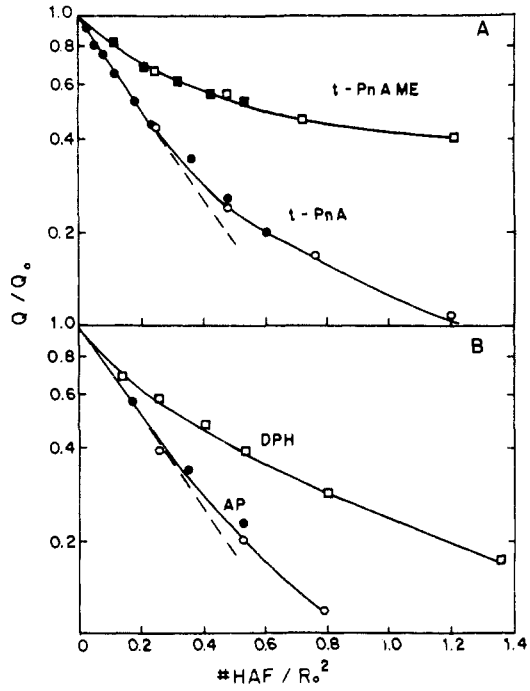

FIGURE 6: Energy transfer in LDL. The data are plotted as the ratio of the donor quantum yield in the presence of acceptor to the donor quantum yield in the absence of acceptor (Q/Q_0) on a logarithmic scale vs. the acceptor surface density expressed as the number of acceptors per R_0^2. Samples contained either 0.0308 mg/mL (in 2.5 mL) total LDL (open symbols) or 0.308 mg/mL total LDL (filled symbols). Surface area calculations are based on the LDL molecular weight of 2.3×10^6, 21% protein; the radius of this particle is 95.9 Å and the surface area is 115 474 Å^2. In panel A, data are shown for *trans*-PnA (●, ○) and *trans*-PnA methyl ester (■, □) at 25° C. In panel B, data are shown for AP (●, ○) and DPH (□). R_0 values are as described in Table I.

quantum yields of PnA probes are strongly dependent upon temperature and environment, R_0 values range between 25 and 30 Å. In the experiments which follow, R_0 values have been corrected for quantum yield variation.

LDL Energy Transfer. The reduction of the quantum yield of several donor probes bound to LDL by energy transfer to HAF is shown in Figure 6. The data are plotted in a characteristic fashion, log (Q_A/Q_0) vs. the acceptor surface density (expressed as the number of HAF acceptors per R_0^2), as explained under Materials and Methods. The energy transfer from *trans*-PnA and *trans*-PnA methyl ester to HAF is shown in Figure 6A. The initial slope of energy transfer is two- to threefold greater for *trans*-PnA than that observed for

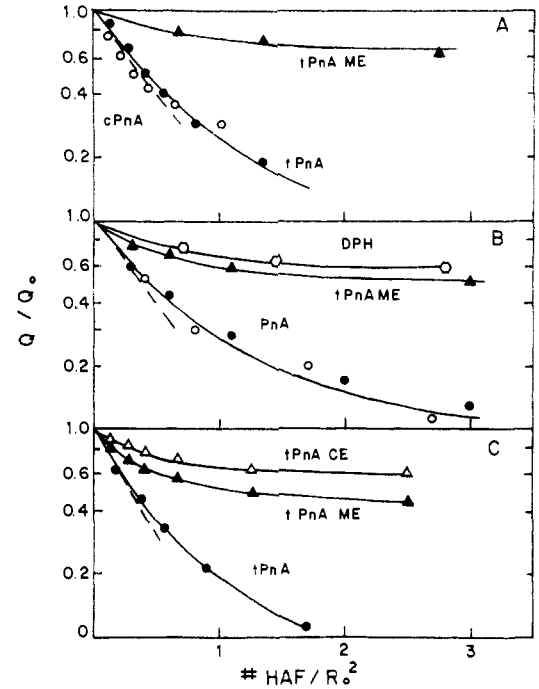

FIGURE 7: Energy transfer in VLDL-size particles at 37 °C. Symbols are *trans*-PnA (●), *cis*-PnA (○), *trans*-PnA methyl ester (▲), *trans*-PnA cholesteryl ester (△), and DPH (□). Panel A: human VLDL from type V hyperlipoproteinemic donor. The sample was obtained by zonal ultracentrifugation and is derived from the first 50 mL of effluent (Patsch et al., 1978). The size range of the particles is estimated from studies of VLDL size ranges (Packard et al., 1979) to be 275 Å in radius. The percent protein in this fraction is similar to that of VLDL from normal donors (J. Patsch, personal communication), i.e., 6.5%. Values for the protein content in these larger VLDL have been reported to be between ~4% and 6.5% (Patsch et al., 1978; Packard et al., 1979; Shen et al., 1977). The sample contained 0.277 mg of VLDL (based on 5.2% protein). Panel B: CER-VLDL; 344-Å radius; composition was 5.8% protein, 18.9% phospholipid, 12.6% free cholesterol, 59.5% cholesterol ester, and 3.1% triglyceride. The sample contained 0.222 mg total. Panel C: model VLDL, triglyceride-rich dispersion (Charlton et al., 1978), contains 60% triolein, 11% cholesterol myristate, 7% cholesterol, 22% DPPC, and ±1% *trans*-PnA cholesteryl ester. The average radius of particles measured from electron microscopy was found to be 325 Å (S. Charlton, personal communication). The sample contained 0.5 mg of lipid total.

trans-PnA methyl ester. Data obtained at two different LDL concentrations which vary by a factor of 10 are nearly coincident. Virtually all of the *trans*-PnA fluorescence may be transferred to HAF whereas the *trans*-PnA methyl ester or cholesteryl ester (not shown) probes exhibit significant residual fluorescence even at high HAF surface density. The behavior of *cis*-PnA and *cis*-PnA methyl ester is comparable to that of the corresponding trans probes (not shown). The energy transfer from another polar donor (AP) and another nonpolar donor (DPH) is similar to that of the polar and nonpolar PnA probes, respectively (Figure 6B). Energy transfer between PnA fatty acid, methyl ester, or cholesteryl ester and HAF is only weakly dependent on temperature (not shown).

VLDL Energy Transfer. Energy transfer measurements in three different VLDL size particles are shown in Figure 7. Transfer efficiency is similar for fatty acid probes (*trans*-PnA) in human VLDL (Figure 7A), CER-VLDL from cholesterol-fed rabbits (Figure 7B), and a model VLDL particle (Figure 7C), all prepared as described under Materials and Methods. In each of these cases, energy transfer from methyl ester probes is considerably less efficient than that from fatty acid probes. The transfer from the nonpolar probes is somewhat less efficient in these large particles than in smaller

LDL particles (Figure 6). Energy transfer from *cis*-PnA is very similar to that from *trans*-PnA (Figure 7A). The transfer from DPH in rabbit CER-VLDL is comparable to that from *trans*-PnA methyl ester (Figure 7B). In the model VLDL particles, energy transfer from cholesteryl ester donors is slightly less efficient than that from methyl ester donors.

Bilayer Energy Transfer. Energy transfer in dimyristoylphosphatidylcholine bilayer vesicles has also been studied (not shown). Energy transfer from the PnA probes, either cis or trans isomers, and fatty acid or methyl ester forms is similar, both above and below the dimyristoylphosphatidylcholine transition. The efficiency is comparable to that observed from the polar PnA (fatty acid) probes in serum lipoproteins when it is taken into account that in a narrow bilayer like dimyristoylphosphatidylcholine, PnA probes in both monolayers probably have their chromophores at similar distances from either surface.

Discussion

Choosing Appropriate Acceptors. Several criteria were applied to the selection of noncovalently bound acceptors for serum lipoproteins. These criteria included (1) the magnitude of the spectral overlap integral, (2) the availability of spectroscopic parameters by which the extent of binding and probe location could be measured, (3) the avidity of binding, and (4) the lack of a detergent effect by the acceptor at the required concentrations. Of several chromophores examined, only HAF fulfilled all of the necessary criteria. The spectral overlap integrals of donors with HAF provide R_0 values of 25–45 Å, a range well suited to lipoprotein energy transfer. HAF binding can be monitored by absorption shifts (Figure 3). Bound HAF was quenched by aqueous iodide differently than was free HAF (Figure 4). HAF did not affect the turbidity of lipoprotein solutions as determined by absorption spectrophotometry. However, several factors must be considered when using HAF: (1) HAF self-quenching (of fluorescence polarization and intensity), characteristic of fluorescein (Pesce et al., 1971) and related to the HAF surface density on lipoproteins, complicates measurements of energy transfer based on HAF acceptor emission; (2) the high polarization anisotropy (0.320) for HAF on LDL reflects significant immobilization and could influence values for the donor–acceptor orientation factor (K^2) and thus R_0, but the combination of the mixed polarization of the acceptor [e.g., Chen & Bowman (1965)][5] and donor motion (DPH and PnA anisotropy is $\sim$0.30) restricts the range of R_0 values (Haas et al., 1978); (3) the absorption spectrum of HAF is strongly dependent upon pH, and since the charge of HAF is affected by pH, its binding properties could be altered.

The location of HAF in LDL is inferred from its accessibility to quenching by aqueous iodide (Figure 4). The linearity of the plot implies that HAF molecules are uniformly accessible, and we conclude that they are found in a single type of environment on the LDL surface. The reduced quenching constant (1.8 M^{-1} for HAF bound to LDL compared to 19 M^{-1} for aqueous HAF monomer) suggests that the fluorescein rings are anchored near the LDL–water interface and partially buried. There are additional chemical factors which make the assignment of the fluorescein rings at the aqueous interface of the particle reasonable: (1) HAF is amphiphilic, containing a polar chromophore attached to a hydrophobic tail; (2) HAF is soluble as monomer only to about 2 μM in either aqueous buffer or hydrocarbon solvents. Therefore, it is with some confidence that we conclude that its several polar substituents anchor HAF to the lipoprotein surface.

Energy Transfer in LDL. The efficiency of transfer from free fatty acid probes, PnA and AP, in LDL is consistent with their location near the particle surface. The depths of the chromophores of these molecules may be estimated by comparison of the initial slopes (dashed lines, Figure 7) with Figure 2B,C. Approximate values of 15 Å for PnA and 25 Å or less for AP are obtained. A further indication of surface location is the extent of quenching at high surface densities. At least 90% of the fluorescence of the fatty acid probes can be transferred to the surface-bound acceptor, HAF. These results are plausible if the fatty acid carboxyl group anchors it to the lipoprotein–water interface with its chain confined to the putative surface monolayer of the lipoprotein particle. The probable orientation of these polar donors would explain why the AP chromophore could be up to 25 Å below HAF at the lipoprotein surface.

In contrast, the efficiency of energy transfer from the nonpolar probes is considerably reduced. The apparent depth of penetration for *trans*-PnA methyl ester is 25–30 Å and for DPH is 40–50 Å, values which may represent their partitioning between the surface and core components of LDL. We have observed that energy transfer for PnA (free fatty acid) and PnA methyl ester probes is similar in dimyristoylphosphatidylcholine and consistent with these chromophores being near the center of the bilayer. Differences in the mobility or orientation of fatty acid and methyl ester probes in a lipoprotein surface cannot therefore account for differences in energy transfer observed in lipoprotein particles. These differences must arise from the penetration of methyl ester probes into the particle interior. For a random distribution of chromophores in a sphere, the volume weighted average depth is the particle radius divided by 4.85 (19.8 Å for a 96-Å LDL particle). Since the surface of LDL probably contains about 50% protein, we expect apparent depths somewhat larger than 19.8 Å to reflect more or less random donor distribution. The analysis is complicated because there is likely to be significant orientation of some of the probes. PnA methyl ester probes may point down from the polar surface and could point out from the nonpolar core.

Packard et al. (1979) report average LDL radii of about 120 Å. When 120 Å is substituted for 96 Å, but the total mass and protein content (21%) are left constant, the number of particles decreases. Although 120-Å particles have increased surface area, the calculated surface area in a lipoprotein sample would decrease by about 20%, thereby increasing the acceptor surface density by 20% but only slightly increasing the apparent donor depth. We should also note that the present analysis does not explicitly consider the influence of surface protein on energy transfer. In the case where protein is distributed on the surface and has dimensions small compared to R_0, the average surface density and distribution of donors and acceptors, and thus energy transfer, will not be strongly altered. When the protein dimensions are large (the extreme situation being the localization of protein on a hemisphere of the lipoprotein surface), the probe molecules are excluded from large regions of the surface (increasing up to twofold the local surface density). However, donors near a lipid–protein boundary will not be surrounded on all sides by acceptors and can have their transfer efficiency reduced twofold or more.[1] Therefore, the effect of increasing probe surface density by restricting probes to a region of the particle surface will be partially offset by the reduced accessibility of some of the

[5] The emission anisotropy of HAF is a strong function of wavelength, crossing through 0.0 in the wavelength region of donor–acceptor spectral overlap.

donors to acceptors. It should be possible to use detailed energy transfer calculations to assess the distribution of lipoprotein apoprotein.

A comparison between energy transfer from PnA and AP serves a further purpose. The motion and orientation of these chromophores are probably considerably different. The motion of PnA, a linear molecule, may be highly anisotropic (Hudson et al., 1978) and described as a "wobble within a cone" (Kawato et al., 1977), with its transition dipole roughly perpendicular to the membrane surface. The motion of the disklike anthroyl chromophore is probably more nearly isotropic (Thulborn & Sawyer, 1978) with its transition dipole able to assume orientations parallel to the surface. The similarity of the energy transfer, after correction for R_0, despite these differences implies that values of the donor–acceptor orientation factor, K^2, probably do not, in this case, play a major role in determining the extent of energy transfer.[6]

Since R_0 for AP is about 50% larger than for PnA, comparable energy transfer is achieved as predicted at surface densities (expressed as the number of HAF per LDL rather than the number of HAF per R_0^2) about threefold less for the AP probes. These results argue that any perturbation of the surface by HAF does not play a significant role in the changes in donor quantum yield observed.

There has been great interest in the thermal reorganization of LDL cholesteryl esters (Deckelbaum et al., 1975, 1977; Atkinson et al., 1977, 1978; Hamilton et al., 1977; Laggner et al., 1977; Muller et al., 1978). We observe only a small effect of temperature on energy transfer in LDL which is probably related to a reduction of R_0 (Table I) as temperature is increased and which reduces the effective depth from which the methyl ester probes may transfer to surface acceptors. We have also studied the temperature dependence of fluorescence polarization of both cis and trans isomers of PnA, PnA methyl ester, and PnA cholesteryl ester in LDL and rabbit CER-VLDL (unpublished experiments). None of the PnA probes detect the melting of the LDL cholesterol esters. These results are in striking contrast to the sensitivity of the parinaric acid probes to the melting of the acyl chains of phospholipid bilayers (Sklar et al., 1979a). These results suggest that the motion on a nanosecond time scale of either surface probe acyl chains or core ester acyl chains is not strongly influenced by the thermal reordering of LDL cholesterol ester sterols.

Energy Transfer in VLDL. For particles as large as VLDL, energy transfer calculated in a planar monolayer (Figure 2A) is a suitable approximation. The chromophores of the PnA (fatty acid) probes are found to be within ~ 0.6–$0.8R_0$ (16–22 Å) from the particle surface. Similar results are found in all three of the VLDL size range particles of differing origin. Energy transfer from the nonpolar donors is significantly less efficient, and their quantum yields are reduced only by about 50% at high acceptor surface densities. This saturation behavior is consistent with the penetration of nonpolar probes into the core of the particle to distances which are inaccessible to energy transfer to HAF and supports the contention that HAF does not penetrate the lipoprotein core (i.e., regions accessible to nonpolar probes only). It appears that DPH partitions more strongly (i.e., "deeper") into the CER-VLDL core than *trans*-PnA methyl ester (Figure 7B) and that *trans*-PnA cholesteryl ester is relatively excluded from the surface of the model VLDL compared to *trans*-PnA methyl ester (Figure 7C). Comparison of results between the particles of different origin is inappropriate because the different constituents of the surface and core of these particles may alter the distribution of nonpolar probes between surface and core.

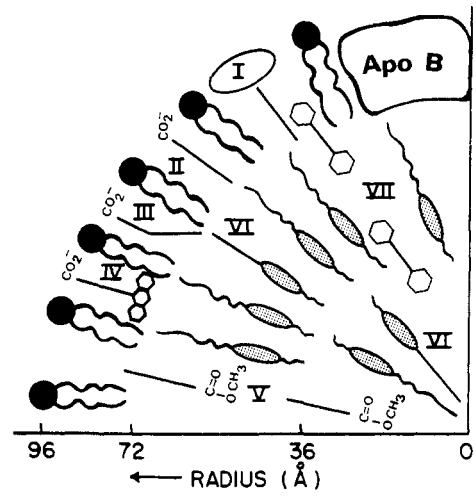

FIGURE 8: Schematic diagram of LDL showing proposed location of several fluorescent probes. LDL is depicted as comprised of a monolayer of phospholipid and protein (cholesterol is omitted) surrounding a core of cholesteryl esters arranged in concentric annuli (triglyceride is omitted). The probes I–VII are identified in the line drawings. The probe species are identified by linear acyl chains.

A qualitative analysis of energy transfer supports a partition of nonpolar probes between surface and core. First, we note that the effective range of energy transfer, even at high acceptor surface densities, is 1–$2R_0$. If *trans*-PnA methyl ester is randomly distributed within VLDL and if we assume that energy transfer with 100% efficiency occurs at the highest accessible acceptor surface densities, but only to distances within $1.5R_0$ from the surface, then, for a particle 250 Å in radius, the volume contained within the spherical shell from 210 to 250 Å (i.e., $1.5R_0$) will be accessible to energy transfer while the interior volume will be inaccessible. The relative volumes of these regions are 41 and 59%, respectively, and are within tolerable agreement with our results.

Conclusions

The conclusions of this investigation are summarized in Figure 8 which shows a simplified section of a low density lipoprotein particle and the proposed location of several fluorescent probes. The primary acceptor, (hexadecanoylamino)fluorescein (I), has its chromophore at the surface of the particle. Fatty acid probes, *trans*-parinaric acid (II), *cis*-parinaric acid (III), and (anthroyloxy)palmitic acid (IV), are anchored, by their carboxyl group, in the surface monolayer of polar lipids and protein. Nonpolar probes, methyl parinarate (V), cholesteryl parinarate (VI), and diphenylhexatriene (VII), are depicted in the core, but significant partitioning between the surface and core of the particle may occur. Although the orientations of these nonpolar probes as depicted are arbitrary, these orientations are likely governed by the organization of the lipids in the core of LDL. The organization of LDL cholesteryl esters will be the topic of a future report. A similar distribution of probes in VLDL is concluded.

While this manuscript was in preparation, another application of fluorescence energy to lipoprotein structure was published (Schroeder et al., 1979). This present report differs in several important respects in that we have defined the location of both donors and acceptors and we have developed a mathematical formalism to interpret energy transfer in lipoproteins. This work represents the primary step—localizing

[6] A number of factors can contribute to the randomization of the donor–acceptor orientation. These factors include the mixed polarization of the acceptor, probe motion, and static contributions which arise from the particle curvature and variable orientation of the probes.

probe molecules—in a rigorous application of fluorescence techniques to lipoprotein structure and metabolism.

References

Atkinson, D., Deckelbaum, R. J., Small, D. M., & Shipley, G. G. (1977) *Proc. Natl. Acad. Sci. U.S.A. 74*, 1042–1046.

Atkinson, D., Tall, A. R., Small, D. M., & Mahley, R. W. (1978) *Biochemistry 17*, 3930–3933.

Berde, C. B., Hudson, B., Simoni, R. D., & Sklar, L. A. (1979) *J. Biol. Chem. 254*, 391–400.

Berlman, I. B. (1971) *Handbook of Fluorescence Spectra of Aromatic Molecules*, Academic Press, New York and London.

Charlton, S. C., Catapano, A. L., Kinnunen, P. K. J., & Lomasky, S. J. (1978) *Fed. Proc., Fed. Am. Soc. Exp. Biol. 37*, 1320.

Chen, R. F., & Bowman, R. L. (1965) *Science 147*, 729–731.

Deckelbaum, R. J., Shipley, G. G., Small, D. M., Lees, R. S., & George, P. K. (1975) *Science 190*, 392–394.

Deckelbaum, R. J., Shipley, G. G., & Small, D. M. (1977) *J. Biol. Chem. 252*, 744–754.

Doody, M. C., Sklar, L. A., Gotto, A. M., Pownall, H. J., & Smith, L. C. (1979) *Biophys. J. 25*, 286a.

Fung, B. K.-K., & Stryer, L. (1978) *Biochemistry 17*, 5241–5248.

Haas, E., Katchalski-Katzir, E., & Steinberg, I. Z. (1978) *Biochemistry 17*, 5064–5070.

Hamilton, J. A., Oppenheimer, N., & Cordes, E. H. (1977) *J. Biol. Chem. 252*, 8071–8080.

Hudson, B., Wolber, P., Tecoma, E., Morgan, C. G., & Simoni, R. D. (1978) *Biophys. J. 21*, 27a.

Jonas, A. (1977) *Biochim. Biophys. Acta 486*, 10–22.

Kawato, S., Kinoshita, K., & Ikegami, A. (1977) *Biochemistry 16*, 2319–2324.

Laggner, P., Degovics, G., Glatter, O., Kratky, O., Kostner, G., & Holasek, A. (1977) *Hoppe-Seyler's Z. Physiol. Chem. 358*, 771–778.

Lowry, O. H., Rosebrough, N. J., Farr, A. L., & Randall, R. J. (1951) *J. Biol. Chem. 193*, 265–275.

Morrisett, J. D., Gallagher, J. G., Aune, K. C., & Gotto, A. M. (1974) *Biochemistry 13*, 4765–4771.

Morrisett, J. D., Pownall, H. J., Roth, R. I., Gotto, A. M., & Patsch, J. R. (1979) *Biophys. J. 25*, 286a.

Muller, K., Laggner, P., Glatter, O., & Kostner, O. (1978) *Eur. J. Biochem. 82*, 73–90.

Packard, C. J., Shepherd, J., Joerns, S., Gotto, A. M., & Taunton, O. D. (1979) *Biochim. Biophys. Acta 572*, 269–282.

Patel, K., Sklar, L. A., Currie, R., Pownall, H. J., Morrisett, J. D., & Sparrow, J. T. (1979) *Lipids 14*, 816–818.

Patsch, W., Patsch, J. R., Kostner, G. M., Sailer, S., & Braunsteiner, H. (1978) *J. Biol. Chem. 253*, 4911–4915.

Pesce, A., Rosen, C., & Pasby, T., Eds. (1971) *Fluorescence Spectroscopy*, p 168, Marcel Dekker, New York.

Rintoul, D., & Simoni, R. D. (1978) *J. Biol. Chem. 251*, 7916–7918.

Schroeder, F., Goh, E. H., & Heimberg, M. (1979) *J. Biol. Chem. 254*, 2456–2463.

Shen, B. W., Scanu, A. M., & Kezdy, F. J. (1977) *Proc. Natl. Acad. Sci. U.S.A. 74*, 837–841.

Sklar, L. A., Hudson, B., & Simoni, R. D. (1975) *Proc. Natl. Acad. Sci. U.S.A. 72*, 1649–1653.

Sklar, L. A., Hudson, B., Petersen, M., & Diamond, J. (1977a) *Biochemistry 16*, 813–819.

Sklar, L. A., Hudson, B., & Simoni, R. D. (1977b) *Biochemistry 16*, 819–829.

Sklar, L. A., Doody, M. C., Gotto, A. M., & Pownall, H. J. (1979a) *Biophys. J. 25*, 286a.

Sklar, L. A., Miljanich, G. P., & Dratz, E. A. (1979b) *Biochemistry 18*, 1707–1716.

Smith, R. J. M., & Green, C. (1974) *Biochem. J. 137*, 413–415.

Stryer, L. (1965) *J. Mol. Biol. 13*, 482.

Tecoma, E. S., Sklar, L. A., Simoni, R. D., & Hudson, B. S. (1977) *Biochemistry 16*, 829–835.

Thulborn, K. R., & Sawyer, W. H. (1978) *Biochim. Biophys. Acta 511*, 125–140.

Wolber, P., & Hudson, B. (1979) *Biophys. J. 28*, 197–210.

Nitrogen-15 Chemical Shifts and $^1J_{^{15}N^1H}$ of Some Tripeptides Measured at the Natural Abundance Level†

J.-P. Marchal* and D. Canet

ABSTRACT: An indirect method combining double-resonance and difference spectroscopy has been used in order to determine ^{15}N chemical shifts and $^1J_{^{15}N^1H}$ in glutathione (in H_2O at pH 3 and under the same conditions with urea added) and in a series of tripeptides of the type Gly-Gly-L-X (with X = Glu, His, Val, Leu, and Ile) in H_2O and at two different pH values. This method has proved to be very efficient as long as the NH proton is not in exchange. The chemical shifts are shown to depend on the considered sequence and especially on the substituent in the γ position. One-bond couplings show some systematic trends which have been tentatively interpreted in terms of the *s* character of the N–H bond. Although these latter parameters seem of potential utility in structural determinations, additional data will be needed in order to rationalize their variations.

Nitrogen-15 chemical shifts have proved shifts to be valuable in the study of small peptides. These parameters provide information about the order of the residues in the sequence (Posner et al., 1975; Markowski et al., 1977; Gattegno et al., 1976; Hawkes et al., 1975). They furthermore allow the study of solvent and/or pH effects (Posner et al., 1975; Gattegno et al., 1976). In a general way, it may be safely assumed that, owing to the importance of nitrogen in molecules of biological

† From the Laboratoire de Chimie Théorique, Université de Nancy I, Case Officielle 140, 54037 Nancy Cedex, France. *Received February 27, 1979; revised manuscript received December 5, 1979.* Equipe de Recherche Associée au CNRS No. 22.

0006-2960/80/0419-1301$01.00/0